An Einstein Model of Brittle Crack Propagation

Brad Lee Holian,[1] Raphael Blumenfeld,[1,2] and Peter Gumbsch[3]
[1]*Theoretical Division, Los Alamos National Laboratory, Los Alamos, New Mexico 87545*
[2]*Cambridge Hydrodynamics, Princeton, New Jersey 08542*
[3]*Max-Planck-Institut für Metallforschung, 70174 Stuttgart, Germany*
(Received 29 July 1996)

We propose a minimal nonlinear model of brittle crack propagation by considering only the motion of the crack-tip atom. The model captures many essential features of steady-state crack velocity and is in excellent quantitative agreement with many-body dynamical simulations. The model exhibits lattice trapping. For loads just above this, the crack velocity rises sharply, reaching a limiting value well below that predicted by elastic continuum theory. We trace the origin of the low limiting velocity to the anharmonicity of the potential well experienced by the crack-tip atom. [S0031-9007(96)02003-0]

PACS numbers: 62.20.Mk, 63.20.Ry

Recent molecular-dynamics (MD) simulations of crack propagation [1,2], as well as experimental studies [3,4], have reflected growing interest in the dynamical aspects of brittle fracture, including the approach to a steady (or quasisteady) state, the buildup of coherent excitation near the crack tip [1,2], and the subsequent onset of instabilities [5,6]. In all of these works, it is fair to say that a coherent, quantitative understanding of the limiting velocity dependence on the local field has not yet been advanced, though many good suggestions have been made [2,7]. Here, we propose a minimal, one-atom, nonlinear model for describing brittle fracture, which we call the "Einstein ice-skater" (EIS) model.

By closely observing movies of MD simulations of brittle crack propagation in a two-dimensional (2D) triangular lattice, under tensile (transverse, or mode I) loading and at zero initial temperature, we noticed that cracks appear to advance as a sequence of essentially one-particle moves. Along the natural cleavage direction separating a pair of close-packed planes (lines in 2D), bond-breaking events are well separated in time [8], which can be characterized as a zigzag, ice-skating kind of motion between the two lines of atoms. When a bond breaks, the forward partner moves ahead, approximately along the former bond direction, while the rearward partner swings back to its final equilibrium position (see Fig. 1). This led us to speculate that the steady-state velocity of a brittle crack could be well approximated by a single-particle Einstein cell model, where the mobile crack-tip atom (the EIS in Fig. 1) moves in a field of six immobile neighbors (the sixth, with whom the bond has just been broken, is assumed to be beyond the range of interaction). The bond-breaking event launches the EIS approximately along the bonding direction. This compressive, nonlinear event results in a shearing motion along the transverse pair of close-packed lines at $\pm 60°$ to the propagation direction, and gives rise to the local vibrational excitations that build up around the crack tip and move coherently with it [1,8].

For sufficiently large strains, the EIS reaches a point that stretches the next bond to breaking after a time t_{break} since the last bond-breaking event. The pattern then repeats—to the other side of the ice-skating phase—and the crack has then advanced by one nearest-neighbor spacing r_0 along the forward direction in the time $2t_{\mathrm{break}}$. The crack velocity is thus given by

$$v_{\mathrm{crack}} = r_0/2t_{\mathrm{break}} . \tag{1}$$

To find t_{break}, we start from the configuration of the EIS and its five connected nearest neighbors and solve for the time dependence of the distance r_{01} between the EIS and its neighbor No. 1; t_{break} is the first time that r_{01} reaches the breaking point r_{max}. The equation of motion for the position $\mathbf{r}_0$ of the EIS (atomic mass m) is

$$m\ddot{\mathbf{r}}_0 = -\sum_{i=1}^{6} \partial\phi(r_{0i})/\partial\mathbf{r}_0 , \tag{2}$$

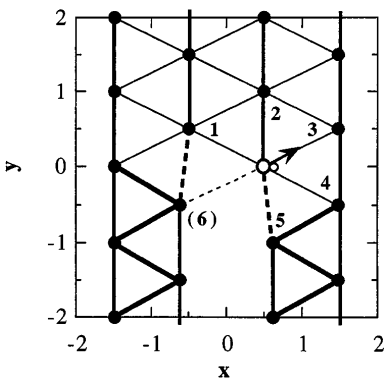

FIG. 1. Initial atomic coordinates for crack propagation in a triangular-lattice strip, four close-packed lines wide; the outer two lines of atoms are fixed, while the inner two are mobile. Heavy lines indicate equilibrium (nearest-neighbor) bonds of length $r_0 = 1$; heavy dashed lines are slightly stretched, nearly vertical bonds; light lines are bonds elastically stretched to length $r_1 \approx 1 + 3\epsilon/4$ by the uniaxial strain ϵ in the x direction; the light dashed line is a just-broken bond with neighbor No. 6. The EIS atom is indicated by the large open circle: it moves initially approximately in the direction of the arrow, stretching the bond with neighbor No. 1 until breakage, then heads toward its final equilibrium position (small circle).

 0031-9007/96/78(1)/78(4)$10.00 © 1996 The American Physical Society

which can be solved given the pair potential $\phi(r_{0i}) = \phi(|\mathbf{r}_0 - \mathbf{r}_i|)$ and the initial conditions. This equation is not trivial to solve, even for harmonic potentials, but can be solved numerically. We first assume the initial EIS coordinates $x = a/2$, $y = 0$ and velocities $\dot{x} = \dot{y} = 0$ (the initial velocities of steady-state crack-tip atoms in full MD simulations are observed to be indeed very small). With $r_0 \equiv 1$, the six immobile neighbors are assumed to be located at $(-a/2, 1/2)$, $(a/2, 1)$, $(3a/2, 1/2)$, $(3a/2, -1/2)$, $(a/2 + a_0\epsilon, -1/2)$, and $(-a/2 - a_0\epsilon, -1/2)$, where $a_0 = \sqrt{3}/2$, $a = a_0(1 + \epsilon)$, and ϵ is the uniaxial strain in the transverse direction to crack propagation. (See Fig. 1.)

We can obtain a crude estimate for t_{break} by imagining that the EIS starts at the turning point of its motion in the final harmonic equilibrium well. The bulk Einstein model is characterized by a frequency of $\omega_E = \sqrt{3}\,\omega_0$, where ω_0 is the fundamental frequency given by $m\omega_0^2 = \phi''(\mathbf{r}_0)$. Hence, if the time t_{break} is one-half the period (from one turning point to the other at bond breaking), then $v_{\text{crack}} = \sqrt{3}\, r_0\omega_0/2\pi$. Since the triangular-lattice shear-wave speed $c_s = \sqrt{3/8}\, r_0\omega_0$ (which is very close to the Rayleigh, or surface wave speed [9]), $v_{\text{crack}}/c_s \approx \sqrt{2}/\pi = 0.45$, independent of the anharmonicity of the potential. Since the effective frequency of a stretched anharmonic bond decreases (actually to zero at the inflection point), the crack velocity in the anharmonic case should be lower.

To go beyond this estimate, we investigated two kinds of attractive snapping-bond potentials: harmonic (HSB) and anharmonic (ASB), the latter based on the Morse potential

$$\phi(r) = (1 - e^{-\alpha(r-1)})^2/2\alpha^2. \tag{3}$$

Here we scale the distance by r_0 and the energy by $mr_0^2\omega_0^2$; α is the repulsive parameter (the familiar Lennard-Jones 6-12 potential is closely approximated by $\alpha = 6$; most materials can be represented by $4 \le \alpha \le 6$). The ASB potential is obtained from Eq. (3) by flattening it out at $r_{\max} = 1 - \ln(1 - \sqrt{\chi})/\alpha$ in the attractive region (beyond the minimum of the Morse potential); the cohesive energy is then $\chi/2\alpha^2$, for $\chi < 1$. The ASB force jumps discontinuously at this point from a negative value to zero—hence the term "snapping bond." For small displacements about $r = 1$, Eq. (3) is approximately harmonic, $(r - 1)^2/2$. The HSB potential cuts off at the same energy as the ASB, but at $r_{\max}^0 = 1 + \sqrt{\chi}/\alpha < r_{\max}$. We find that *the range and maximum attractive force of the potential are the essential parameters that govern the crack velocity.*

Our choice of snapping-bond potentials makes precise the definition of the distance beyond which a bond is considered "broken," an ambiguous concept for completely continuous potentials. Since our goal is to compare this EIS model with a fully dynamical system, a well-defined breaking point for both is a distinct advantage. The fully dynamical systems we compare with are rather restrictive, namely, close-packed lines of atoms of width $w = 4, 8, 16$, and 64, with the outer two clamped, and the inner free to move; moreover, only nearest-neighbor interactions are considered. (Strips were typically $200r_0$ in length; steady-state propagation is attained well within 10% of that length.)

For this thin-strip, fixed-grip geometry, the critical Griffith strain ϵ_G for initiating forward crack motion can be computed by equating the potential energy in two transverse sections of the strip of height $r_0/2$: one far behind the crack with all bonds in equilibrium, except for the one broken bond, and the other far in front, with all bonds equally stretched. The Griffith criterion is obtained from

$$(w - 1)\phi(r_1) = \phi(r_2) = \chi/2\alpha^2, \tag{4}$$

where r_1 is the elastically stretched bond ($r_1^2 = a^2 + 1/4$) and r_2 is the broken bond across the gap of the relaxed crack. The Griffith criterion ϵ_G is thus

$$\epsilon_G = \begin{cases} \left\{1 - \frac{8}{3\alpha}\ln\left(1 - \sqrt{\frac{\chi}{w-1}}\right)\left[1 - \frac{1}{2\alpha}\ln\left(1 - \sqrt{\frac{\chi}{w-1}}\right)\right]\right\}^{1/2} - 1, & \text{ASB} \\ \left\{1 + \frac{8}{3\alpha}\sqrt{\frac{\chi}{w-1}}\left[1 + \frac{1}{2\alpha}\sqrt{\frac{\chi}{w-1}}\right]\right\}^{1/2} - 1, & \text{HSB}. \end{cases} \tag{5}$$

An intriguing aspect of the EIS model is the straightforward emergence of the lattice-trapping phenomenon [10]: unless the strain exceeds a value well above ϵ_G, the distance between the EIS and its neighbor No. 1 will not reach $r_{\max}$. The strain must therefore exceed ϵ_G by a barrier amount of overstrain that is a characteristic of the atomistic nature of the crack tip, and which can only be evaluated atomistically. In Fig. 2, we show our results for the crack-tip velocity (in units of c_s), as a function of the strain, for the EIS model and for the fully dynamical $w = 4$ strip ($\alpha = 6, \chi = \frac{1}{2}$). The EIS model agrees to within 10% of the velocity with the MD results—remarkable for such a simple model.

However, the lattice-trapping strain is underestimated by 13% for the anharmonic and 12% for the harmonic system, which is most clearly due to neglected correlations with farther neighbors in the EIS model. For the anharmonic system, the onset of crack motion for the fully dynamical $w = 4$ strip occurs at a crack velocity of about 30% of the shear-wave speed, while for the

harmonic system, the crack starts at about 50% of the shear-wave speed. Under further loading, the crack-tip velocity increases roughly linearly with strain but with a higher slope for the harmonic than for the anharmonic system.

To compare our EIS results to MD simulations and experiments we rescaled the wider system strains by the Griffith strain ($\epsilon_G \sim 1/\sqrt{w}$) and found good agreement, except for slight, but systematic increases in the lattice trapping strain with size for harmonic potentials. We can understand this by noting that wide anharmonic systems, where stretched bonds weaken, are more compliant and tend to have local strains near the crack tip that are closer to those in the narrow strips. On the other hand, harmonic bonds do not weaken with stretching, so that the global strains is spread more democratically across the system. We emphasize that, even in wide systems where the global strain can be arbitrarily small, the fact that local strains near the crack tip are large (of order 10%, as in the narrow-strip case) is a significant reason for the success of the EIS model.

We find that crack velocities in anharmonic systems are essentially independent of the anharmonicity parameter, at least over the range $4 \leq \alpha \leq 6$; in fact, the curves for $\alpha = 4$ and 5 practically overlap. As the cohesive strength χ decreases from $\frac{1}{2}$ down to $\frac{1}{8}$ (along with the range of the potential), crack velocities in anharmonic systems show a slight increase ($\sim$10%) in ultimate slope and greater variability in the jump-off lattice-trapping strain. (In the limit $\chi \to 0$, of course, the harmonic limit is approached [7].) In general, velocities in anharmonic systems are lower than in harmonic ones, show less variation with strain, and exhibit relatively lower lattice trapping (when the strain is scaled by ϵ_G). Similar trends are exhibited in the full MD simulations, including those using full, continuous (rather than discontinuous snapping-bond) potentials [1,2,7,8], and those for systems much wider than $w = 4$. Again, the principal differences are in the lattice-trapping strains. We can therefore conclude that the EIS approximates very well the crack-tip atomic motion, just as our intuition from larger-scale MD simulations had suggested.

Our minimal EIS model indeed confirms speculations about the correlation of the limiting steady-state crack-tip velocity and anharmonicity [2,7,8]. The more "realistic" anharmonic interactions give steady-state crack-tip velocities that never exceed 0.4 of the Rayleigh speed, in excellent agreement with experimental observations [3,4]. With the EIS model, the origin of this low speed can clearly be attributed to the smaller attractive force on the crack-tip atom at the point of bond breaking, as compared to the harmonic (or linear elastic) analysis.

Under loading, the thin-strip MD crack-tip velocity in Fig. 2 jumps sharply at the lattice-trapping strain to a slowly rising linear regime, and then once again rises sharply at a strain of $0.15 = 1.3\epsilon_G$. Close examination of atomic configurations revealed that this second rise

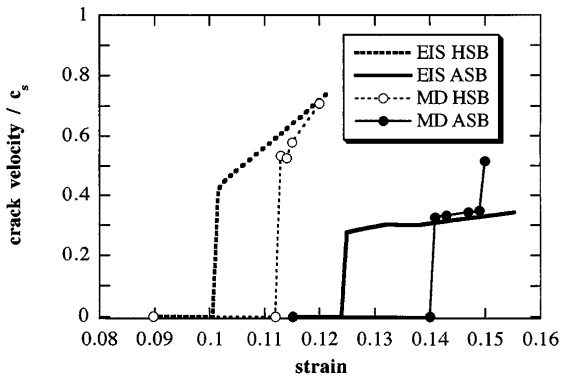

FIG. 2. Crack velocity (in units of shear-wave speed c_s) as a function of strain for the anharmonic snapping-bond (ASB) and harmonic snapping-bond (HSB) potentials. Results for the EIS model are shown for Morse parameter $\alpha = 6$ and cohesive bond-strength $\chi = \frac{1}{2}$, along with $w = 4$ strip MD simulations (closed circles for ASB and open for HSB).

is associated with two instabilities: the first is a wake of large-amplitude surface (Rayleigh) waves behind the crack tip; at somewhat higher strains, the crack begins to jump from the central channel to one of the side channels next to the fixed-grip atoms (see Fig. 1). We have observed this zigzag propagation by plus or minus one channel in much wider systems, where, at even higher strains, dislocations are emitted, followed immediately by branching. Dynamical instabilities such as these divert energy from brittle bond breaking, causing the crack-tip velocity to drop rather than rise. Dislocation emission and real crack branching are, of course, forbidden processes in the artificially narrow 4-wide strip, and are completely absent in the one-particle EIS model.

Finally, the hysteresis under unloading and healing up of the crack can be obtained from the EIS. To do this, we simply detect when the 6-neighbor model reconnects the bond between the EIS atom and neighbor No. 6, rather than opening up the crack in the forward direction. This occurs soon below ϵ_G for the anharmonic potential (namely, $0.98\epsilon_G$), but substantially lower for the harmonic potential ($0.85\epsilon_G$). Crack propagation and crack healing are thus quite asymmetric processes.

In conclusion, the Einstein ice-skater model of brittle crack propagation is able to predict quantitatively the steady-state crack velocity under loading, including lattice trapping, as well as hysteresis upon unloading and crack healing. The maximum velocity achieved in full MD simulations as a function of strain is principally limited by the anharmonicity in the attractive region of the pair potential, which is captured by the EIS; however, it is also affected by instabilities that involve collective motion (energy buildup, dislocation emission, and branching), which is inaccessible to the one-particle EIS model. Nevertheless, this simple EIS model allows us to explain, in quite satisfactory quantitative fashion, the effect of nonlinear motion of the crack-tip atom on the limiting crack velocity.

We thank Robb Thomson, Shujia, and Bill Hoover for stimulating discussions.

[1] B. L. Holian and R. Ravelo, Phys. Rev. B **51**, 11 275 (1995); S. J. Zhou, P. S. Lomdahl, R. Thomson, and B. L. Holian, Phys. Rev. Lett. **76**, 2318 (1996).

[2] P. Gumbsch, in *MRS Symposium Proceedings: Fracture—Instability Dynamics, Scaling, and Ductile/Brittle Behavior,* edited by R. L. Blumberg Selinger, J. J. Mecholsky, A. E. Carlsson, and E. R. Fuller, Jr. (Materials Research Society, Pittsburgh, 1996), Vol. 409, p. 297; see also P. Gumbsch, in *Computer Simulation in Materials Science,* edited by H. O. Kirchner, L. Kubin, and V. Pontikis (Kluwer Academic, Dordrecht, Netherlands, 1996), p. 227.

[3] W. G. Knauss and K. Ravi-Chandar, Int. J. Fract. **27**, 127 (1985).

[4] J. Fineberg, S. P. Gross, M. Marder, and H. L. Swinney, Phys. Rev. Lett. **67**, 457 (1991); E. Sharon, S. P. Gross, and J. Fineberg, Phys. Rev. Lett. **74**, 5096 (1995).

[5] M. Marder and S. Gross, J. Mech. Phys. Solids **43**, 1 (1995); E. S. C. Ching, J. S. Langer, and H. Nakanishi, Phys. Rev. Lett. **76**, 1087 (1996); E. Sharon, S. P. Gross, and J. Fineber, Phys. Rev. Lett. **74**, 5096 (1995); **76**, 2117 (1996).

[6] R. Blumenfeld, Phys. Rev. Lett. **76**, 3703 (1996); F. Lund, Phys. Rev. Lett. **76**, 2724 (1996).

[7] K. Sieradzki, G. J. Dienes, A. Paskin, and B. Massoumzadeh, Acta Metall. **36**, 651 (1988); K. Sieradzki and R. Li, Phys. Rev. Lett. **67**, 3042 (1991).

[8] P. Gumbsch, S. J. Zhou, and B. L. Holian, Phys. Rev. B (to be published).

[9] W. T. Ashurst and W. G. Hoover, Phys. Rev. B **14**, 1465 (1976).

[10] R. Thomson, Solid State Phys. **39**, 1 (1986).